



# Tin Electrodeposition from Sulfuric Acid Solution Containing Nigella Sativa Essential Oil Added

Benabida Abdelillah  
Ibn Tofail University, MOROCCO

Mohammed Cherkaoui  
Ibn Tofail University, MOROCCO

Received 28 April 2016 • Revised 15 September 2016 • Accepted 16 September 2016

## ABSTRACT

Experimental investigations have been performed, using cyclic and linear sweep Voltammetry, to determine the effects of Nigella sativa essential oil additive (NS) on the electrodeposition of tin on mild steel in acid sulfuric solution. The experiments were performed under different plating time, different current densities, pH and temperature conditions. Tin electrodeposition on mild steel was performed using a DC - supply at denoted operating parameters. The presence of the NS additive caused an increase of the activation energy and of the overvoltage of the reduction of hydrogen and stannous ions. The surface of the plated steel was examined using Scanning electron microscope. Different surface characteristics were obtained depending upon the presence or free-additive. The electrodeposition rate of the plated surface was also determined by a gravimetric technique. The quality of the electro-deposition of tin, in the presence of Nigella sativa, was good as indicated by the microstructural morphology of the plated surface except for the few porosities demonstrated.

**Keywords:** tin, nigella sativa essential oil, electrodeposition, mild steel, deposition rate

## INTRODUCTION

There is a concern, which is more and more accentuated, for the use of the tin as a substitute for the conventional depositions because of its more safe impact upon the environment [1-3]. For example, the tin and the tin alloys are the potential alternatives for the replacement of the chrome and cadmium depositions that are utilized for some decorative means and in the electronic applications respectively [4].

The electrodeposition of the tin can be performed both by the acid baths and also by the basic baths [5,6]. However, Tin and its alloys could be electrodeposited from different electrolytes, thorough aqueous fluoroborate, sulfate, and methanesulfonate solutions [7-9]. Porous or dendritic deposits are commonly obtained. A lead compound is often added to hinder the reduction of the stannous species and increase the polarization reaction [7].

© **Authors.** Terms and conditions of Creative Commons Attribution 4.0 International (CC BY 4.0) apply.

**Correspondence:** Benabida Abdelillah, *Laboratory of materials, electrochemistry and environment, Faculty of Science, Ibn Tofail University, PB 133-14050 Kénitra, Morocco.*

✉ [benabida2000@hotmail.com](mailto:benabida2000@hotmail.com)

In addition to that, the hydrogen codeposition usually leads to many undesirable effects in metal deposition. To dodge pollution and hydrogen evolution problems, organic additives, or surfactants are ordinarily used to ameliorate the deposit morphology.

The benefit in using natural organic compositions is on account of its availability, price and impact on the environment [10-13]. They pose no harmful effect on the environment or danger to human health. A number of natural organic compounds have been specified as good brightening factors in tin electroplating. These classes of organic compounds are biodegradable and non-toxic [14]. One of these substances is *Nigella sativa* essential oil (NS).

Seeds of *Nigella sativa* L. (black cumin or black seeds) are closely used in traditional Islamic medicine and for culinary intention worldwide. *Nigella* seed essential oil is becoming vulgar in and out of the Islamic world. Composition of *Nigella* seed essential oil is known to be location- following. Due to, previous investigations regarding *N. sativa* seed essential oil composition or yield have reported large variations [15], possibly resulting from a different plant geographical origin, Where, the investigation of the chemical composition of *N. sativa* seed essential oil cultivated in Morocco, then the essential oil was prepared by solvent- or cold press-extraction [16]. Characteristic features of the seed essential oil founded a high degree of unsaturation and as confirmed by gas chromatography reported herein, the main unsaturated fatty acids were linoleic acid followed by oleic acid, while the main saturated fatty acid was palmitic acid [16]. Oxygen atoms is present in their molecular structures and in addition, linolenic and linoleic acids include double bonds, which form a potential adsorption sites on the mild steel surface by the donation of electrons to the empty d-orbital of Iron. Their relative percentages are reported in **Table 1**.

**Table 1.** Chemical composition of *Nigella sativa* essential oil from Morocco<sup>17</sup>

Constituent	%
Linoleic acid	58.5
Oleic acid	23.8
Palmitic acid	13.1

In this work we will study the electrochemical behaviour of Sn(II) in sulphuric bath with NS as additive at 298 K using mild steel working electrode. Cyclical and linear sweep Voltammetry has been applied for qualitatively testing tin-electrolyte systems. The effect of process variables such as electrodeposition rate, current density, pH and temperature, will be investigated further.

## EXPERIMENTAL METHODS

### Materials, techniques and Solutions

The **Table 2** give the standard bath compositions for Sn deposits. The solutions were processed using distilled water and reagent grade chemicals. The bath temperature for electrodeposition was 298 K. The electrochemical measurements were performed in a three

**Table 2.** Composition of studied baths

Electrolytes	SnSO <sub>4</sub> (M)	H <sub>2</sub> SO <sub>4</sub> (M)	NS additive (ppm)
a	0.14	0.56	0
b	0.14	0.56	10

electrode cell using mild steel electrode as working (area=1cm<sup>2</sup>), a platinum wire as counter electrode and Ag/AgCl/KCl (3M) as reference electrode. Prior to every experiment, the surface of the working was abraded employing emery paper up to 1500 grade and then being immersed in pure ethanol, and distilled water, respectively, to take away any surface impurity.

Various electrochemical techniques were used. Cyclic, linear, and stripping voltammograms were registered at potential scan rate of 10 mV.s<sup>-1</sup>. First cyclic voltammetry (CV) sweep was always performed from the initial potential of 1.2 V (Ag/AgCl) towards more negative values. Stripping analysis was performed immediately after potentiostatic tin deposition at fixed potential without removing the working electrode from the solution. Anodic stripping curves were registered from deposition potentials up to 1.2 V. Galvanostatic method was also used for electrodeposition studies at various constant currents densities. Volta lab (Radiometer PGZ 100) controlled by a microcomputer was applied in all measurements.

### Gravimetric measurements

Gravimetric experiments in the basic solutions (**Table 2**) without and with NS additive were carried out using rectangular mild steel coupons having the same purity as for mild steel rods. The dimensions of the coupons were 1.0 cm length, 1.0 cm width, and 0.20 cm thickness. The coupons were polished and dried as for mild steel rectangular, weighted (initial weight,  $m_{int}$ ). After exposure to the designated test solution, the samples were rinsed with distilled water, washed with acetone to remove a possibly formed film due to the additive, dried between two paper silk, and weighing again (final weight,  $m_{fin}$ ). The deposition rate ( $v$ ) during the time of exposure were calculated as follows [17-21]:

$$v = \frac{\Delta m}{\Delta t \cdot S \cdot \rho_{s_n}} \quad (1)$$

where  $\Delta m$  is the gain mass of the substrate (g),  $S$  is the substrate surface (cm<sup>2</sup>),  $\rho_{s_n}$  is the tin density (g/cm<sup>3</sup>) and  $\Delta t$  is the polarization time of the working electrode (s).

## RESULTS AND DISCUSSION

### Galvanostatic polarization

The **Figure 1** shows the transient of a solution of sulfate tin and sulfuric acid in the presence and absence of NS additive for optimal current density of 15 mAcm<sup>-2</sup> on the steel electrode. After a delay inherent in the adsorption kinetics of the NS additive to the surface, we notice that the electrodes immersed in the electrolyte containing the additive are

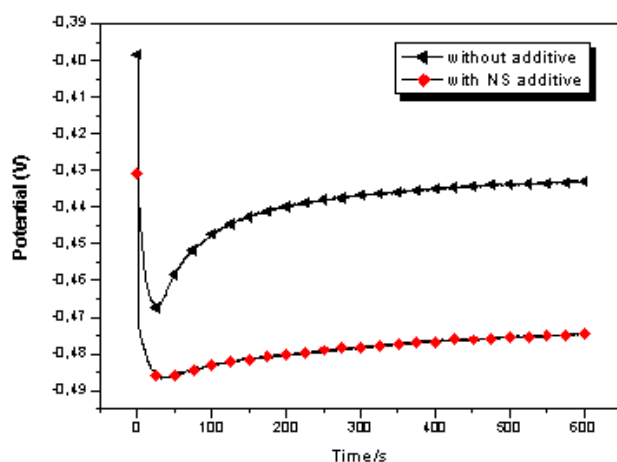


**Figure 1.** Tin reduction, in the presence and in the absence of the NS additive, by galvanostatic polarization with current density of  $-15\text{mA}\cdot\text{cm}^{-2}$  at  $25^\circ\text{C}$

significantly more cathodic potential in its absence. For a constant applied current intensity, the addition of NS additive moved the cathodic reduction potential of the system. This is one of the most interesting, because most deposits are made in galvanostatic mode and the introduction of such an overvoltage may contribute to achieving codeposition with an element having a potential of more cathodic reduction [22].

### Linear sweep Voltammetry and cyclic Voltammetry

The cathodic polarization curves of tin deposition on steel cathodes were recorded potentiodynamically in the presence and without NS additive were measured in the basic solution (Table 2). The potentiodynamic measurements were swept from the rest potentials in the negative potential direction with scan rate of  $10\text{mV}\cdot\text{s}^{-1}$ . (Figure 2) Generally, the deposition of tin from sulfuric acid baths is characterized by high polarization, and appearance of cathodic peak C at the deposition potential of tin. The cathodic peak C is assigned to the discharge of the  $\text{Sn}^{2+}$  ions (4). The result obtained show that, in the presence of NS, the drop in the cathodic current, after the peak potential of the peak C indicates suppression of hydrogen evolution [23]. Such attitude can be attributed to the formation of an obstruct Sn hydroxide formed and adsorbed on a cathode surface. It is probable that some of the progression sites for hydrogen are occupied by adsorbed Sn hydroxide. On the other hand, the hydrogen gas evolution is more inhibited compared to the case without the additive. It appears that parts of the surface become blocked to tin deposition, perhaps due to the high concentration of adsorbed blocking NS additive, as well as the formation of whiskers became very limited [14, 24].

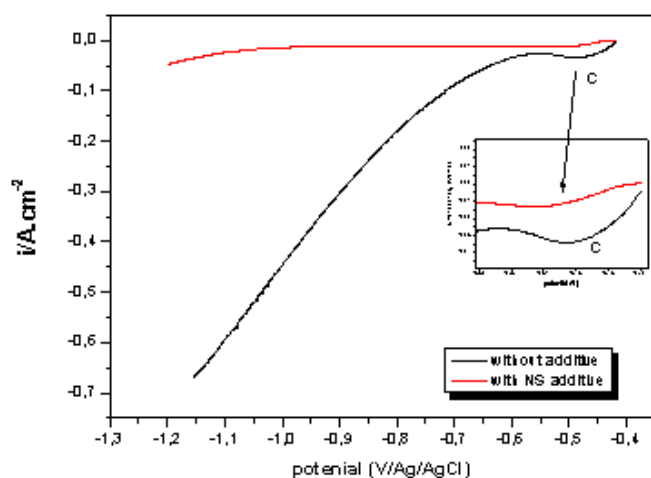


**Figure 2.** Cathodic polarization curves of 0.14M SnSO<sub>4</sub> + 0.56M H<sub>2</sub>SO<sub>4</sub> with and without NS additive at 10 mV.s<sup>-1</sup> and 25°C

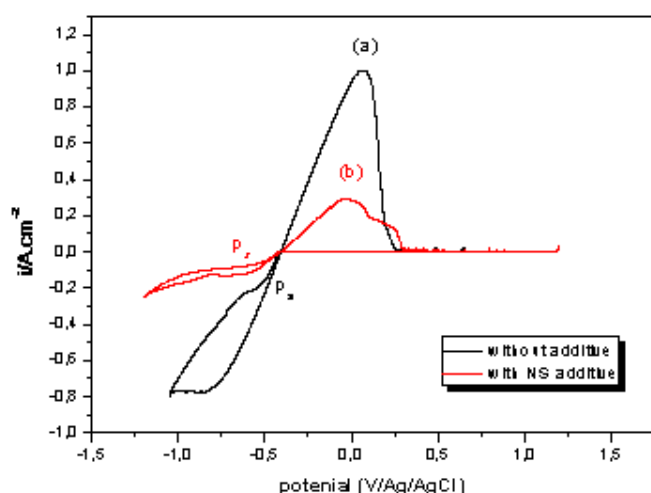


**Figure 3.** Cyclic Voltammetry curves of 0.14M SnSO<sub>4</sub> + 0.56M H<sub>2</sub>SO<sub>4</sub> with and without NS additive, at 10 mV.s<sup>-1</sup> and 25°C

The influence of this additive on deposition of Sn was also studied operating cyclic voltammetric method. **Figure 3** shows the typical voltammograms obtained from the optimized bath solutions in the presence and without NS additive with a scan rate of 10 mV.s<sup>-1</sup>. The main information about the Sn coating and the structure of the deposited phases is given by the voltammetric response.



The voltammogram (curve a) has a peak  $p_a$  reduction potential at  $E = -520$  mV/Ag/AgCl corresponding to the formation of the tin deposit. This current peak is followed by a diffusion bearing highlighting the kinetically controlled by diffusion. The value of the

current density, which occurs this level, gives us the value of the current limit. From the potential  $E = -600 \text{ mV} / \text{Ag/AgCl}$ , occurs an increase in current accompanied by a release of gas at the cathode. The tin deposit being formed, the substrate is no longer in contact with the solution. The increase in current corresponds to the evolution of hydrogen (5) on the tin deposit. The return scan, more rugged is characterized by the absence of intersection with the forward scan. This lack of sprouting loop shows that the metal deposition does not occur by a three-dimensional germination (3D). The return curve is also marked by a cathodic-anodic current transition characterizing rapid dissolution of the deposit [22].



The addition of the NS additive in the electrolyte  $\text{SnSO}_4 + \text{H}_2\text{SO}_4$  radically changes the shape of the voltammogram (curve b). The very precise steps and characteristics of the tin electrocrystallisation are clearly visible. Cathodic part characterized by a very low current and a peak reduction  $P_z$  at  $-620 \text{ mV} / \text{Ag/AgCl}$ . In the presence of NS additive, the  $P_z$  peak reduction of tin species seems to be moving towards more cathodic potentials. Indeed, this peak is similar to the peak obtained without additive, but with a shift in potential of  $100 \text{ mV/Ag/AgCl}$ . In this area of potential occurs a very low gas emission corresponding to a slight evolution of hydrogen. This peak  $P_z$  therefore relates to the deposition of tin under the influence of the additive that induces crystallization overvoltage. Scanning return is comparable to that obtained without additive, but with a lower current. While tin only has the characteristics of rapid dissolution, tin in the presence of NS additive is more akin to a slow dissolution system indicating that the additive plays a role of corrosion inhibitor [22].

### Deposition rate

The deposition rate ( $v$ ) at various current densities applied was determined using the gravimetric technique (3). It was established, from **Figure 4a**, that the electrolytic bath without additive gives a relatively low deposition rate, between  $5 \mu\text{m} / \text{h}$  to  $25 \mu\text{m} / \text{h}$ . However, the presence of NS additive to the basic aqueous solution improve the deposition rate, which corresponds to typical values of  $27$  to  $40 \mu\text{m} / \text{h}$ . This tremendous improvement in deposition rate shows the important role that can play the NS additive for electroplating tin. Furthermore, the presence of NS additive in the tin bath may lead to inhibit the rate of the hydrogen evolution reaction. Suppression of HER can substantially increase the current efficiency [25]. From a certain current density, the deposits become spongy, and the whiskers are beginning to appear on the surface of the electrode, this may explain the decrease in the deposition rate (**Figure 11**).

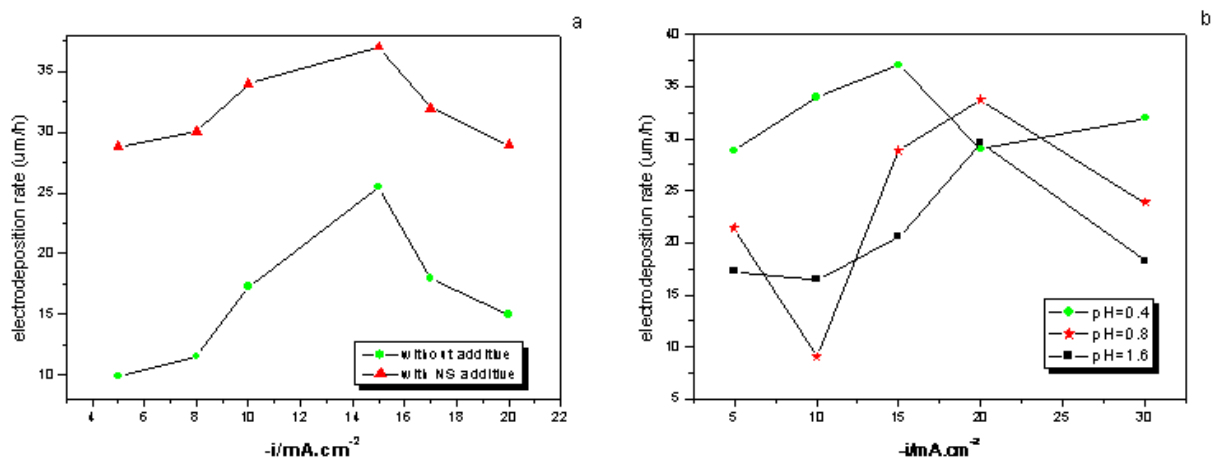


**Figure 4.** (a) Current density effect in electrodeposition rate with and without additive at pH= 0.4. (b) Current density effect in electrodeposition rate with NS additive at different pH values

The electrodeposition tin is performed in an acid bath, but the degree of the acidity can influence on the quality of the plating and tin plating average. Thus, the solution pH is a significant factor in the electrodeposition, indeed, it affects both anodic and cathodic reactions and various phenomena correlating with the structure and composition of the metal-solution interphase. The major phenomena include; adsorption, potential zero charge, structure of the double layer, structure of ion species in the solution and the ionic strength of the solution [26]. The **Figure 4b** shows the deposition rate as a function of various applied current densities at different pH values. It is shown that, the deposition rate improves as the medium is more acidic, while there is a weakness of deposition rate with increasing pH in the bath. The tin deposit is more preferable in acidic medium. In addition, during the current density range studied, 15  $\text{mA}\cdot\text{cm}^{-2}$  remains optimal for the high deposition rate for different acidities, and when this value is exceeded, it is shown that the rate of deposit begins to decrease.

The galvanostatic polarization corresponding electroplating tin with and without NS additive, that have enabled access to the deposition rate, is shown in **Figure 5**. The three transient curves shows a rapid decrease, then a slow stabilization. The result proves that the overvoltage has increased in absolute value, with increasing pH, for different current densities of 10  $\text{mA}\cdot\text{cm}^{-2}$  to 20  $\text{mA}\cdot\text{cm}^{-2}$ . This process became clearer in **Figure 6**, when we plot the potential vs. pH.

Conforming to The Butler-Volmer equation (4), the electrical current on the electrode associated with the electrode potential, considering that both a cathodic and an anodic reaction occur at the same electrode. As the current increases, the voltage drop will increase, which leads to the increase of the polarization (overvoltage  $\eta$ ) and as a consequence the increase of the number of nucleation [27, 28].

$$I = A \cdot i_0 \cdot \left\{ \exp \left[ \frac{(1 - \alpha) \cdot n \cdot f}{R \cdot T} \cdot (E - E_{eq}) \right] - \exp \left[ - \frac{\alpha \cdot n \cdot f}{R \cdot T} \cdot (E - E_{eq}) \right] \right\} \quad (4)$$

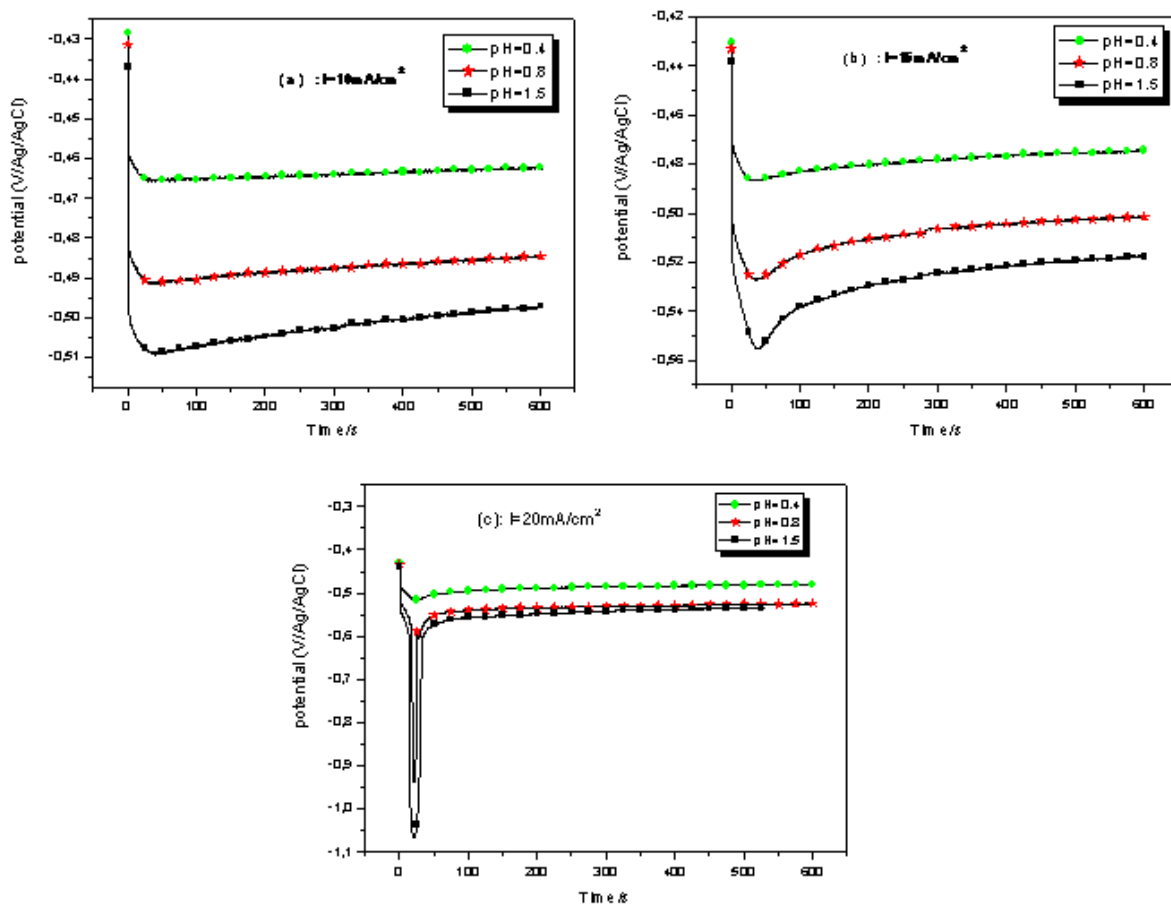


**Figure 5.** Potentiostatic current-time transients during tin deposition in the presence of NS additive, at different current densities

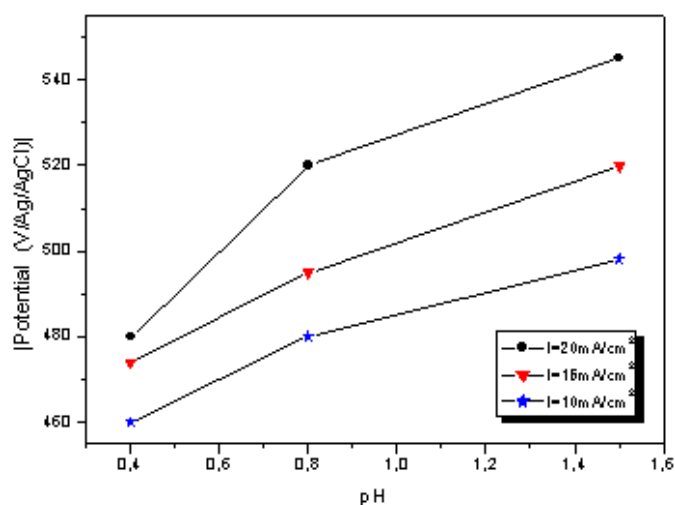


**Figure 6.** pH effect on overvoltage, at different current densities, in the presence of NS additive, during the galvanostatic polarization



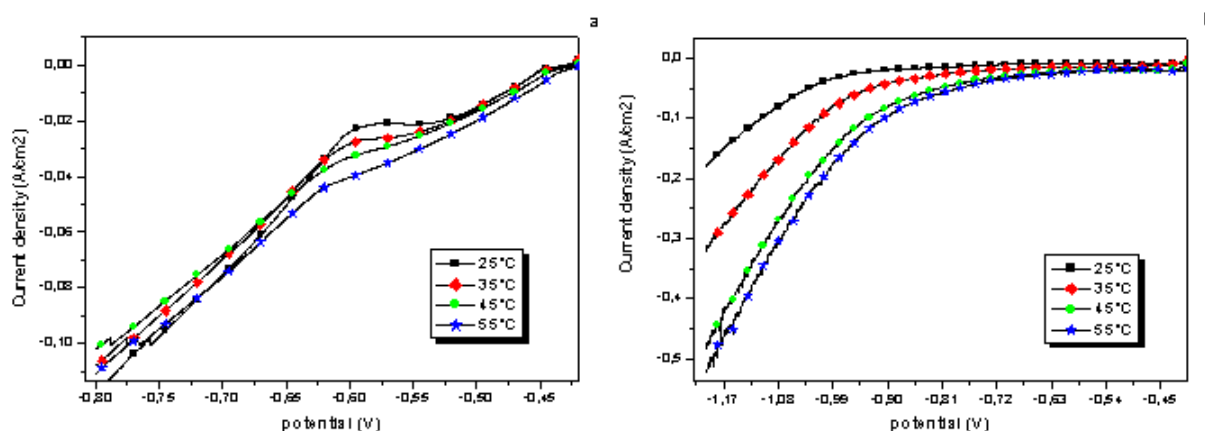


**Figure 7.** Electrodeposition of tin, recorded at various temperatures, at a scan rate of  $10 \text{ mV}\cdot\text{s}^{-1}$ , from the electrolyte. (a) without additive. (b) with NS additive

where  $I$  is the electrode current,  $i_0$  is the exchange current density,  $E$  is the electrode potential,  $E_{eq}$  is the equilibrium potential,  $A$  is the electrode active surface area,  $n$  is the number of electrons involved in the electrode reaction,  $T$  is the absolute temperature,  $F$  is the Faraday constant,  $\alpha$  is the charge transfer coefficient.  $R$  is the universal gas constant.

In fact, the overvoltage is a complex parameter. According to Vetter [29], It can be separated in four additive terms charge transfer overvoltage  $\eta_t$ , diffusion overvoltage  $\eta_d$ , reaction overvoltage  $\eta_r$ , and crystallization overvoltage  $\eta_{cr}$ . At first sight, only the crystallization overvoltage should be taken into consideration. Furthermore, It is difficult to measure and a more detailed analysis shows that It is also necessary to take into account the charge transfer, the diffusion and the eventual reaction overvoltages because they may impact the local distribution of the current density and also the equilibrium concentration of metal atoms (i.e., metal atoms diffusing at the surface of the crystal before being integrated in the lattice) at the surface of the metal [30].

The result shown in **Figure 6** may be explained by considering that the decrease in acidity is accompanied by the diminishing of hydrogen ions in the solution, which hinders its reduction to dihydrogen  $\text{H}_2$ , therefore, this might encourage the  $\text{Sn}^{2+}$  ion transfer across the electrical double layer, and leads to overvoltage generation on the electrode surface.

### Temperature effect

The voltammograms of the **Figure 7** shows the effect of NS additive and temperature on the reduction of tin and especially the hydrogen evolution. When there was no additive (**Figure 7a**), hydrogen evolution took place around  $-0.60\text{V}$  versus  $\text{Ag}/\text{AgCl}$ ; with NS added, hydrogen evolution occurred at a more negative potential ( $\sim -0.82 \text{ V}$ ). This increase in hydrogen overpotential (**Figure 7b**) was due to the inhibitory impact of NS on hydrogen evolution [31]. On the other hand, it appears that, at a given potential, the current density

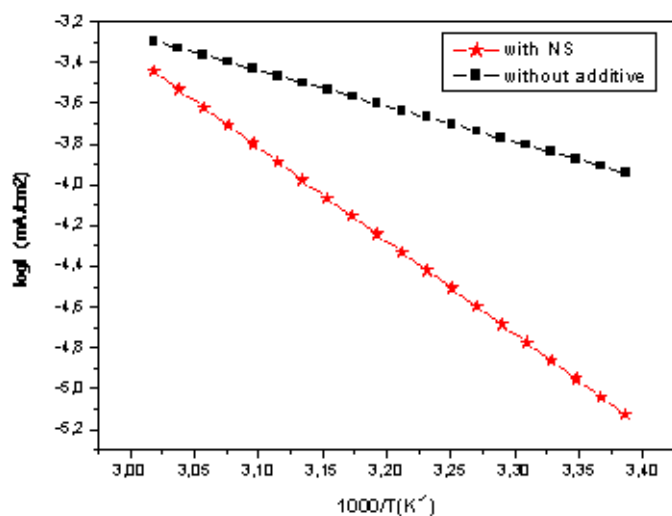


**Figure 8.** Logarithm of the current density versus  $T^{-1}$  for the electrodeposition of tin at a potential of -570 mV. Data taken from [Figure 7](#)

**Table 3.** The value of activation energy for carbon steel in 0.56 M  $H_2SO_4$  in the absence and presence of  $10^{-4}$  M of NS additive

	Linear regression coefficient (r)	$E_a$ (kJ/mol)
Without additive	0.99964	14.54
With NS additive	0.99877	38

increases with increasing temperature. Each temperature increase produces a clear change in the experimental lines that move to negative areas where accelerates hydrogen evolution [32].

$$\frac{d(\log(i))}{d(\frac{1}{T})} = -\frac{E_a}{2.3 * R} \tag{5}$$

where  $i$  is the current density limit,  $E_a$  is the activation energy,  $R$  is the universal gas constant, and  $T$  is the absolute temperature.

The lines representing the limiting current density versus the reciprocal temperature, are shown in [Figure 8](#). Using Arrhenius Equation (5), the calculation of the energy of activation from the slope of these lines was proven to increase from 15  $kJ.mol^{-1}$  without additive to 38  $kJ.mol^{-1}$  in the presence of NS additive. This augmentation confirms the blockage of the surface of the working electrode by molecules of the NS additive [33]. Furthermore, the increase of  $E_a$  may also suggest a decrease of the diffusion coefficient of  $Sn^{2+}$  ions in the bath with added NS oil [34].

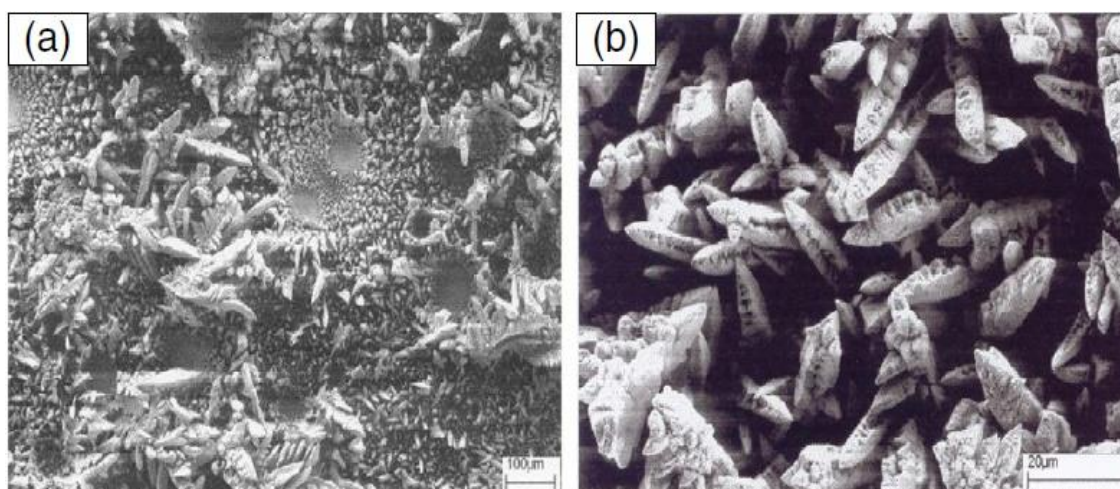


**Figure 9.** SEM images of tin deposits obtained at 25°C from the additive-free bath under the current density of 15 mA.cm<sup>-2</sup>

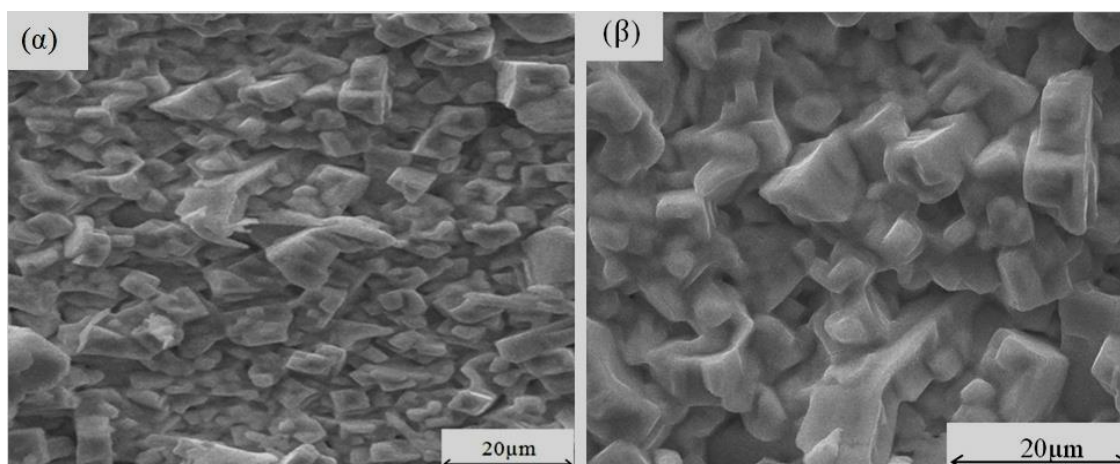


**Figure 10.** SEM images of tin deposits obtained at 25°C in the presence of 10 ppm of NS additive bath under the current density of 15 mA.cm<sup>-2</sup>

### SEM morphology

The surface morphology of the deposited tin from baths with NS, and NS-free, under 15 mA.cm<sup>-2</sup>, pH = 0.4, 25°C and  $\Delta t = 10$  min was examined by scanning electron microscopy (SEM) and the results are displayed in **Figure 9** and **Figure 10** respectively. The results obtained revealed that the electrodeposited tin in the absence of NS, is mainly composed of a small compact and homogeneous needle-like crystals not covering the entire cathode surface (**Figure 9a** and **b**). However, the addition of NS to the plating bath leads to the formation of smaller and more compact grains, and the particles begin to cluster (**Figure 10α** and **β**). Moreover, the presence of microcracks, in the deposit, indicates that the deposits, in the case of the absence of NS, are highly stressed as a result of hydrogen evolution during deposition [35].

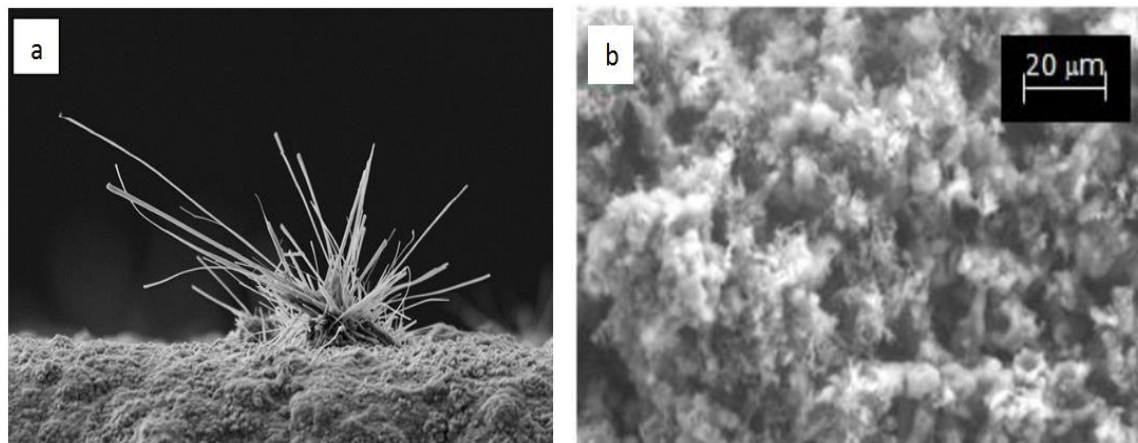


**Figure 11.** SEM images of the whiskers and the spongy tin deposits obtained on the surface of the electrode

## CONCLUSIONS

Tin have been electrodeposited from an aqueous sulfuric acid electrolyte in the presence and without Nigela Sativa essential oil under different parameters and conditions. The cyclical and linear sweep Voltammetry have confirmed the effect of the NS additive on the kinetics during the process of reduction and dissolution of forming metal. It was found that the presence of the examined additive induced an increase of the activation energy and of the vervoltage of the reaction of stannous and the hydrogen evolution. NS additive for use as an addition agent gave a good electrodeposition of tin with thin, dense and Close- packed crystal grains on the mild steel surface in the sulfuric acid tin solution. Characterization of the tin plated surface of the mild steel substrate showed a different surface morphology depending on plating conditions. The electrodeposition process is sensitive to changes in pH and applied current density. Although not as bright as the NS essential oil bath, the surface structures obtained indicate that the tin coating can serve many useful purposes of protection that could be technologically and economically viable, as well as it is non-toxic and environmentally friendly.

## REFERENCES

1. Sabitha, R., Pushpavanam, M., Mahesh Sujatha, M. & Vasudevan, T. (1996). Electrodeposition of tin from tartrate solutions. *Trans. Met. Finish. Ass*, 5, 267.
2. Sheppard, K. G. (1996). Abstracts of the 190-th Meeting of the Electrochemical Society. *The Electrochemical Society Pennington, NJ*, 306 - 395.
3. Vitkova, S. & Young Yang, B. (1994). An electrochemical study on Zn- Sn-alloy-coated steel sheets deposited by vacuum evaporation. *Part I. Surf. Coating Tech.*, 64, 99.
4. Strafford, K. N. & Reed, A. (1984). Coatings reduce the fouling of microfiltration membranes. *Coat. and Surf. Treat. for Corr. and Wear Resist*, 74.
5. Smirnov, M. I., K.M, T. & Popov, A. N. (1995). Effect of organic surfactants on the kinetics of electrodeposition of tin and tin-lead alloy from methanesulfonic electrolyte. *Russ. J. Electrochem*, 31, 498.

6. Stirrup, B. N. & Hampson, N. A. (1997). Anodic passivation of tin in buffered phosphate electrolyte. *J. Electroanal. Chem.*, 5, 429.
7. Chen, Y. H., Wang, Y. Y. & Wan, C. C. (2007). Microstructural characteristics of immersion tin coatings on copper circuitries in circuit boards. *Surf. Coat. Technol.*, 202, 417.
8. Low, C. T. J. & Walsh, F. C. (2008). The stability of an acidic tin methanesulfonate electrolyte in the presence of a hydroquinone antioxidant. *Electrochim. Acta*, 53, 16.
9. Park, Y. W., Sankara Narayanan, T. S. N. & Lee, K. Y. (2007). Effect of temperature on the fretting corrosion of tin plated copper alloy contacts. *Wear*, 262, 320.
10. Schlesinger, M. & Paunovic, M. (2011). *Modern electroplating*, 5<sup>th</sup> Ed., John Wiley & Sons.
11. Loto, C. A. (1993) Effect of sugar cane and cassava juices as addition agents in the electrodeposition of zinc from acid based solution. *Discov. Innovat.*, 5, 253.
12. Loto, C. A., Olefjord, I. & Mattson, H. (1991). The Effect of Mango Bark and Leaf Extract Solution Additives on the Corrosion Inhibition of Mild Steel in Dilute Sulphuric Acid-Part 1. *Corros. Prevent. Contr.*, 39, 885.
13. Loto, C. A., Olefjord, I. & Mattson, H. (1992). Effect of inhibitors and admixed chloride on electrochemical corrosion behavior of mild steel reinforcement in concrete in seawater. *Corros. Prevent. Contr.*, 39, 149.
14. Tripathy, B. C., Singh, P., Muir, D. M. & Das, S. C. (2001). Effect of organic extractants on the electrocrystallization of nickel from aqueous sulphate solutions. *J. Appl. Electrochem.*, 31, 301.
15. Benabida, A., Galai, M., Zarrouk, A. & Cherkaoui, M. (2014). Effects of linseed oil additive on the electroplating of tin on mild steel. *Der Pharma Chemica*, 6, 285-293.
16. Cheikh-Rouhou, S., Besbes, S., Hentati, B., Blecker, C., Deroanne, C., Attia, H. (2007). *Food Chem*, 101, 673-681.
17. Gharby, S., Harhar, H., Guillaume, D., Roudani, A., Boulbaroud, S., Ibrahim, M., Ahmad, M., Sultana, S., Ben Hadda, T., Chafchaoui-Moussaoui, I. & Charrouf, Z. (2013). Chemical investigation of *Nigella sativa* L. seed oil produced in Morocco. *Journal of the Saudi Society of Agricultural Sciences*, 14(2), 172-177.
18. Sherif, E. M. & Park, S.-M. (2006). Effects of 2-amino-5-ethylthio-1, 3, 4-thiadiazole on copper corrosion as a corrosion inhibitor in aerated acidic pickling solutions. *Electrochim. Acta*, 51, 6556.
19. Sherif, E. M. & Park, S.-M. (2006). Inhibition of copper corrosion in acidic pickling solutions by N-phenyl-1, 4-phenylenediamine. *Electrochim. Acta*, 51, 4665.
20. Sherif, el-S. M., Erasmus, R. M., Comins, J. D. (2007). Corrosion of copper in aerated acidic pickling solutions and its inhibition by 3-amino-1, 2, 4-triazole-5-thiol. *J. Colloid & Inter. Sci.*, 306, 96.
21. Sherif, el-S. M. (2012). [PDF] Electrochemical and gravimetric study on the corrosion and corrosion inhibition of pure copper in sodium chloride solutions by two azole derivatives. *Int. J. Electrochem. Sci.*, 7, 1482-1495.
22. Bakkali, S., Tour, R., Cherkaoui, M. & EbnTouhami, M. (2015). Influence of S-dodecylmercaptobenzimidazole as organic additive on electrodeposition of tin. *Surface and Coatings Technology*, 261, 337-343.
23. Soto, F. & Crousier, J. (1998). Electrocrystallisation de revêtements zinc-manganèse: comportement à la corrosion, s. n. theses.fr.
24. Abd El Rehim, S. S., et al. (1998). Anomalous electrodeposition of zinc-nickel alloys from aqueous citrate baths. *J. Metall*, 52, 304-308.
25. Nuñez, M. (2005). *Metal electrodeposition*, Nova Publishers.
26. Anik, T., Ebn Touhami, M., Himm, K., Schireen, S., Belkhamima, R. A., Abouchane, M. & Cissé, M. (2012). Influence of pH solution on electroless copper plating using sodium hypophosphite as reducing agent. *Int. J. Electrochem. Sci.*, 7, 2009-2018.

27. Yu, J., Cao, H., Chen, Y., Kang, L. & Yang, H. (1999). A new approach to the estimation of electrocrystallization parameters. *J. Electroanal. Chem.*, 69, 474.
28. Chassaing, E. & Wiart, R. (1992). Electrocrystallization mechanism of Z- Ni alloys in chloride electrolytes. *Electrochim. Acta.*, 37, 545.
29. Vetter, K. J. (1961). *Experimentelle Ergebnisse der elektrochemischen Kinetik. Elektrochemische Kinetik.* Springer Verlag, 698.
30. Winand, R. (1994). Electrodeposition of Metals and Alloys---New Results and Perspectives. *Electrochimica Acta*, 39, 1091-1105.
31. Wen, S. & Szpunar, J. A. (2005). Nucleation and growth of tin on low carbon steel. Nucleation and growth of tin on low carbon steel. *Electrochimica Acta*, 50, 2393-2399.
32. Miles, M., Kissel, G., Lu, P. & Srinivasan, S. (1976). Effect of temperature on electrode kinetic parameters for hydrogen and oxygen evolution reactions on nickel electrodes in alkaline solutions. *Journal of the Electrochemical Society*, 123, 332-336.
33. Pasquale, M. A., Gassa, L. M. & Arvia, A. J. (2008). Copper electrodeposition from an acidic plating bath containing accelerating and inhibiting organic additives. *Electrochimica Acta*, 53, 5891-5904.
34. Abd El Rehim, S. S., Ibrahim, M. A. M., Dankeria, M. M. & Emad, M. (2002). Electrodeposition of amorphous cobalt-manganese alloys on to steel from gluconate baths. *Trans. IMF*, 80, 105.

**<http://iserjournals.com/journals/ejac>**